Effect of gypsum addition on acid resistance of Ye'elimite rich calcium sulfoaluminate cement

Tom Damion, Piyush Chaunsali

PII: S0958-9465(23)00409-2

DOI: https://doi.org/10.1016/j.cemconcomp.2023.105335

Reference: CECO 105335

To appear in: *Cement and Concrete Composites*

Received Date: 22 November 2022

Revised Date: 6 August 2023

Accepted Date: 13 October 2023

Please cite this article as: T. Damion, P. Chaunsali, Effect of gypsum addition on acid resistance of Ye'elimite rich calcium sulfoaluminate cement, *Cement and Concrete Composites* (2023), doi: https://doi.org/10.1016/j.cemconcomp.2023.105335.

Effect of Gypsum Addition on Acid Resistance of Ye'elimite Rich Calcium Sulfoaluminate Cement

Tom Damion and Piyush Chaunsali*

Department of Civil Engineering, Indian Institute of Technology Madras, Chennai, India

*Corresponding author: pchaunsali@iitm.ac.in

Abstract

Calcium sulfoaluminate (CSA) cements exhibit useful properties such as shrinkage compensation and rapid strength development. Acid resistance of CSA cement is majorly governed by its phase composition that varies significantly depending on the desired properties. In this study, acid resistance of CSA cement (i.e., non-expansive) and gypsum blended CSA cement (i.e., expansive) is explored. The current work emphasizes that a small change in phase assemblage can cause large difference in the performance under acidic environment. Conventional acid immersion tests with hydrochloric acid (HCl) of 1% and 2% conc., and sulfuric acid (H_2SO_4) of 2.95% conc. were considered in the study. Furthermore, a recently developed acid consumption method was used to rank the binders with regard to their acid resistance in HCl and H_2SO_4 environments. It was found that the gypsum blended CSA cement showed poorer performance than CSA cement in acidic environment despite having marginally higher compressive strength before acid exposure.

Keywords: Acid Neutralisation Capacity; Hydrochloric Acid; Sulfuric Acid; Calcium Sulfoaluminate Cement; Gypsum

1 Introduction

Calcium sulfoaluminate (CSA) cements and other sustainable binders are currently being explored due to the need to reduce carbon footprint and energy requirement associated with construction industry. CSA cement manufacturing involves 25 – 35% lower CO_2 emission as compared to Portland cement [1]. In this work, acid resistance of CSA binder having varying amounts of gypsum is evaluated. Acid attack is a major durability problem in chemical warehouses, agricultural industries, and sewer structures, where it is also referred to as biogenic acid attack [2–4]. As a result of acid attack, strength-loss and mass-loss occur, leading to the area-loss of constructed elements [5].

It was observed that surface spalling and microstructure degradation were directly proportional to the water-to-cement ratio (w/c) in case of sulfate attack of CSA binders [6]. In a study by [7] the best performance in mechanical properties was observed with an optimised ye'elimite content of 30 – 40% and w/c ratio of about 0.35 – 0.50. The study also reported an increase in the ettringite content with an increase in w/c and ye'elimite content. Strätlingite is a minor phase which is formed due to the reaction between belite and amorphous aluminium hydroxide. The amount of strätlingite was found to be inversely proportional to the gypsum content and directly proportional to w/c ratio [8].

On incorporating gypsum into CSA clinker, the ratio of ettringite-to-monosulfate increases. As per a study [9], gypsum addition delayed the hydration of belite and ferrite phases; reduced the amount of strätlingite and pore solution; and increased the compressive strength. When the gypsum/ye'elimite ratio (M-value as per [10]) was low, less ettringite was formed along with the formation of strätlingite in presence of surplus aluminium [9]. Gypsum blending has been reported to accelerate the hydration of synthesised ye'elimite [11]. However, the effect of additional gypsum blending on hydration kinetics of ye'elimite containing sufficient calcium sulfate could not be distinguished [12]. A reduction in cumulative heat of hydration upon gypsum addition has been reported due to dilution effect [13]. In presence of gypsum, lower amount of amorphous content is formed. Hydrated assemblage of synthesised ye'elimite (87.9% ye'elimite, 6.7% anhydrite, 5.1% CA[1], and 0.3% CA_2) had microcrystalline AH_3 (gibbsite-like)[14]. However, when gypsum was blended, low-density amorphous type AH_3 was formed [13]. Such an amorphous aluminium hydroxide has higher surface area than the crystalline one (5 – 380 times) [13]. This points to the higher water content in amorphous AH_3 [13,15] and its potential to bind sulfate [16]. Amorphous aluminium hydroxide is stable till pH 3 – 4 on acid attack [17,18] and offers a high neutralisation capacity (Eq. 1) [19,20]. Even acid resistance of calcium aluminate cement has been attributed to AH_3 phase's high neutralisation capacity [21–23] and the stability of calcium aluminate hydrate phases [24].

$$Al_2O_3.3H_2O + 6H^+ \rightarrow 2A1^{3+} + 6H_2O \quad (1)$$

[1] Cement chemistry notation C= CaO, A = Al_2O_3, S = SiO_2, $\hat{S}$ = SO_3, H = H_2O

Ettringite-based high alumina cement systems have been reported to degrade more than Portland cement system in acetic acid (pH of 3 and 5) and nitric acid (pH of 3) [25]. Depending on the composition of CSA binder, the proportion of phases such as ettringite, monosulfate, aluminium hydroxide, strätlingite, and C-S-H vary [26,27]. Hence, acid resistance of CSA binder will be greatly affected by its phase composition. In a study, PC was reported to have slightly higher hydrochloric acid (HCl) resistance than CSA cement (ye'elimite: 29%, calcium sulfate: 5.3%, belite: 55.2%) [28]. However, the statistical significance of the difference was not clear. The salts formed in HCl attack (i.e., $CaCl_2$ and $AlCl_3$) have high solubility. As a result, HCl attack is characterised by extensive decalcification. Low calcium CSA-PC blend are expected to have lower decalcification and reduced formation of gypsum. The performance (measured through altered depth) of CSA cement and PC-CSA blend was found to be better than PC [29]. In an in-situ sewer exposure experiment reported by [30], it was found that CSA cement outperformed sulfate resisting Portland cement. Under exposure to sulfuric acid of pH 2, the deterioration was characterised by gypsum deposition at early period of exposure and H^+ ion attack at later period [31]. The acid resistance has been found to be influenced by the acid type. In a study by Damion et al. [32], CSA cement was outperformed by PC in 1% sulfuric acid solution, whereas CSA cement performed better than PC in citric acid (0.5 M) attack because of the higher amount of tri-calcium di-citrate hexahydrate (expansive in nature) formed in PC [32]. When different criteria such as mass-loss and unaffected core area fraction were considered, the organic acid resistance of CSA cement (CaO: 44.4%, SO_3: 8.7%, Al_2O_3: 31.75%, SiO_2: 10.7%) seemed to be different in case of citric, lactic, acetic, and butyric acids [20,33]. Variable composition of CSA cement poses challenge in predicting its acid resistance. Previous studies on comparative performance of CSA cements having non-expansive and expansive characteristics are scarce. Controlled addition of gypsum to CSA cement can transform it into an expansive binder, which has potential application in shrinkage-compensation. This study aims at evaluating acid resistance of a high ye'elimite CSA cement (with and without external gypsum) in two different acidic environments. Furthermore, a short-period acid consumption test using an autotitrator was utilized to evaluate the acid resistance of cementitious binders.

2 Materials and methods

A commercially available CSA cement was used in this work. The CSA cement (specific gravity of 2.86) was a rapid hardening and non-expansive binder. The oxide composition of the CSA cement is shown in the Table 1.

Table 1 Oxide composition (% by weight) of CSA cement

SiO_2	CaO	Al_2O_3	SO_3	Fe_2O_3	MgO	K_2O	TiO_2	SrO	Na_2O	LOI*
14.0	39.8	20.9	14.5	3.6	2.8	0.5	1.1	0.1	0.2	1.8

* Loss on ignition

Powder X-ray diffraction (XRD) was performed to determine the phase composition of CSA cement. Table 2 shows the phase composition (of 100% crystalline content) obtained through quantitative X-ray diffraction analysis.

Table 2 Phase composition (% by weight) of CSA cement

Phases/Binder	Amount (%)
Ye'elimite	35.5
Anhydrite	15.5
Gypsum	1.5
Lime	3.9
Dicalcium silicate	28.7
Dolomite	7.6
Brownmillerite	3.5
Mayenite	2.1
Quartz	1.7

2.1 Specimen preparation

Prismatic specimens of dimensions 10 mm × 10 mm × 60 mm were cast to monitor the mass, dimensional changes, and the characterization thereafter. For determining compressive strength,

50 mm × 50 mm × 50 mm paste cubes were cast. Two water-to-cement ratios (w/c) of 0.5 and 0.6 (by weight) were considered and distilled water was used for casting. The effect of gypsum blending was studied by adding 15% gypsum based on previous works in the area [11,12,34]. Table 3 shows the mix proportions used in the study. The mixing procedure for the specimens used in strength test was carried out in accordance with ASTM C305-06 in a front-mounted planetary Hobart mixer. The mixing for prisms used in acid exposure was performed using a high-shear paste mixer. Specimens were cured for 28 days at 25°C and 65% relative humidity environment.

Table 3 Mix proportions (by wt. %) of binders

Terminology	CSA-HY	Gypsum	w/c
HY 0.6	100%	0	0.6
HY+15G 0.6	85%	15%	0.6
HY 0.5	100%	0	0.5
HY+15G 0.5	85%	15%	0.5

2.2 Acid attack tests

For acid immersion tests, the solution-to-specimen volume ratio was kept as 20. Three specimens were immersed in 360 ml acid placed inside 500 ml beaker with a specially fabricated glass spacer underneath (Figure 1). The spacer was designed to ensure minimum contact area with specimen allowing maximum acid exposure. The apparatus was covered at top. The specimens were washed in running tap water weekly before measuring changes in mass and dimensions. The pH of neutralised solution was measured weekly before replacement with a fresh acid solution to maintain near uniform pH. The acidic solutions considered in the study were 1% HCl, 2% HCl, and sulfuric acid of pH 0.5, as shown in Table 4. As per ASTM C1898 [35], pH 0.5 was the lowest pH considered in the sulfuric acid immersion tests. The maximum exposure period was limited to 35 days. The entire immersion test was performed in a lab maintained at 25°C (± 2°C).

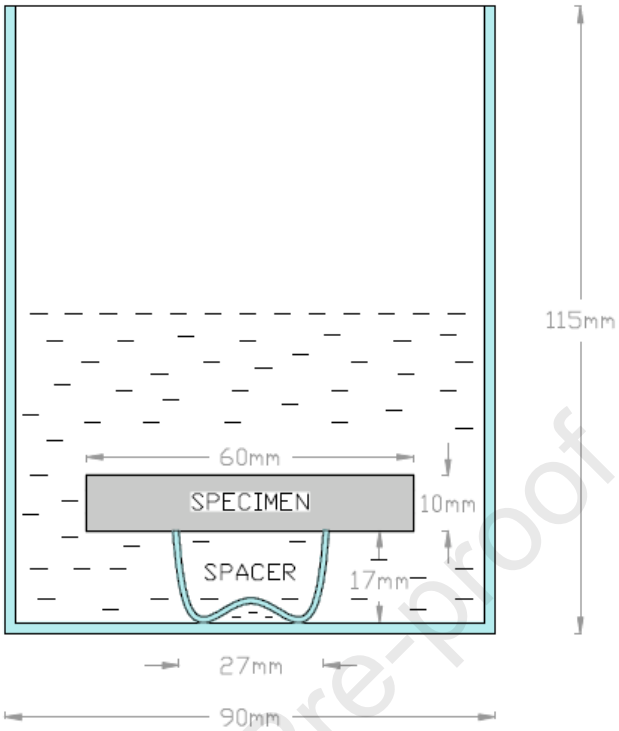

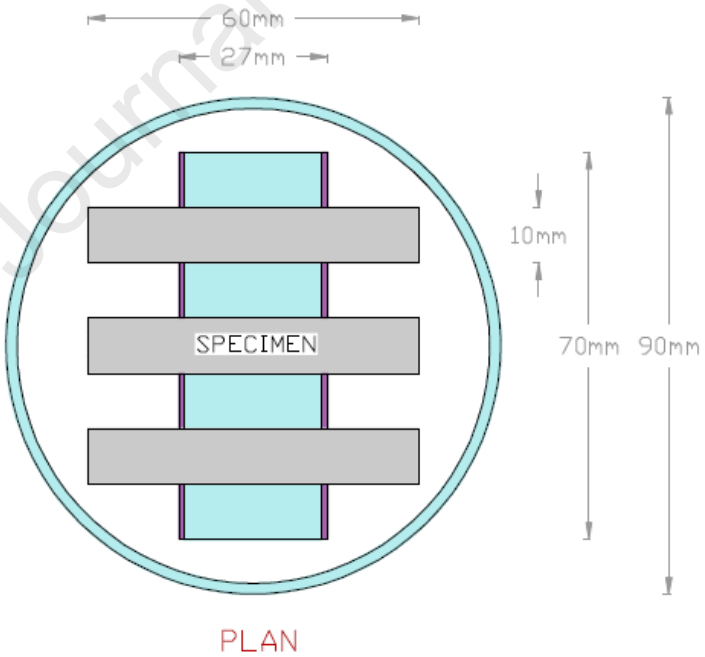

Figure 1 Schematic of exposure set up

Table 4 Details of exposure solutions

Acid and concentration	pH
HCl (1%)	0.59 (±0.01)
HCl (2%)	0.33 (±0.005)
H_2SO_4 (2.95%)	0.50 (±0.01)

2.3 Mass and dimensional changes

Normalized mass at a particular time was taken with respect to the 28-day cured specimen (control). Similarly, normalized cross section area was calculated with respect to the area of control specimen. Cross sectional dimensions of specimens were measured using a digital calliper having a sensitivity of 0.001 mm. The widths and depths at three different locations were measured and the average cross-sectional area was calculated from the measurements.

2.4 Compressive strength

Compressive strengths of paste cubes were determined after 28 days of curing. Compressive strength test was performed at a loading rate of 900 N/s.

2.5 X-ray diffraction (XRD)

X-ray diffraction (XRD) was used to compare the mineralogy of 28-day cured control samples, acid attack products, and to quantify the phase composition of CSA cement. Samples were ground, sieved through 75 μm, before performing XRD. XRD was performed using MiniFlex Rigaku powder X-ray diffraction instrument using Cu Kα *(*wavelength 1.5405 Å). The tube voltage and current were 40 kV and 15 mA, respectively. The diffractogram was collected between the 2-Theta range of 5 – 60° with step size of 0.02° and scanning rate of 0.2 s per step size. For quantitative analysis, pure zinc oxide (ZnO) was used as an external standard. The diffractograms were analyzed using X'Pert HighScore plus software.

2.6 Thermogravimetric analysis (TGA)

Thermogravimetric analysis was performed using LABSYS evo TGA from SETARAM Instrumentation. The test was carried out in the range of 30 °C – 900 °C with heating rate of 15°C/min in a nitrogen-purged environment using alumina crucibles. The sample preparation for TGA was similar to that for XRD, as discussed above.

2.7 Scanning electron microscopy (SEM)

Scanning electron microscopy was performed using FEI-Quanta FEG 200F equipment. Specimens were subjected to gold sputter coating before performing SEM. For the imaging, dwell time was selected as 30 μs, accelerating voltage as 20 kV, beam current as 1 nA, and spot size as 2.5 nm.

2.8 Acid consumption test

The exposure solution pH was measured weekly using the pH electrode (resolution of 0.001 pH) of autotitrator. The acid consumption [36] was determined using the automatic titrator (Metrohm 916 Ti Touch). The apparatus involves an intelligent pH electrode, temperature sensor, acid dosing system and a propeller type stirrer. Ground hydrated binder (size of less than 90 μm) of one gram was mixed with 50 ml of distilled water before titration. The method involved initial 10 min of premixing to obtain a homogeneous suspension imitating pore solution. The stirrer rotated at 900 – 1000 rpm throughout the method and this speed was optimised based on the trials. After premixing, sulfuric acid (5%) was dosed. The solution was continuously stirred to ensure that the measured pH was representative of the entire volume. The titration curve was analysed for various phases.

In order to determine the stabilizing point acid consumption and the divergence point pH, cured monolithic specimens were taken for static pH (STAT) test. Three prismatic specimens were immersed in 250 ml sulfuric acid solution of pH 2 in a 500 ml beaker. The autotitrator was used for maintaining constant pH 2 along with continuous stirring at 450 – 500 rpm speed, thus inducing some dynamic effect. The test was done to collect initial period acid consumption and continued till 12 hours.

3 Results

3.1 Hydration, mineralogy, and strength of CSA-based binders

Hydration of CSA-based binder is governed by the hydration of ye'elimite phase. The chemical reactions involved in the hydration of CSA cement are shown below [26,37,38]:

$$C_4A_3\hat{S} + 18H \rightarrow C_3A.C\hat{S}.12H + 2AH_3 \quad (2)$$

$$C_4A_3\hat{S} + 2C\hat{S}H_2 + 34H \rightarrow C_3A.3C\hat{S}.32H + 2AH_3 \quad (3)$$

$$C_2S + 2H \rightarrow \text{C-S-H (calcium silicate hydrate)} + CH \quad (4)$$

$$C_2S + AH_3 + 5H \rightarrow C_2ASH_8 \text{ (strätlingite)} \quad (5)$$

It is noted that the amorphous aluminium hydroxide is formed in first two reactions. According to reaction (3), the ratio between unreacted gypsum and ye'elimite should be 2.225 [39]. However,

the stoichiometric ye'elimite can react with large amount of water to form ettringite, calcium aluminate hydrate (CAH_{10}), and aluminium hydroxide (as shown in reaction 6) [13]. This reaction, theoretically predicted by thermodynamic calculations, creates discrepancy due to the unreliable data for AH_3 and CAH_{10} [40]. Rather ettringite, monosulfate, and aluminium hydroxide were found to be formed experimentally [40].

$$3C_4A_3\hat{S} + 98H \rightarrow C_3A.3C\hat{S}.32H + CAH_{10} + 2AH_3 \quad (6)$$

Based on the M-value, the hydration reactions can be predicted [41]. When M-value < 2, reaction 3 occurs first, followed by reaction 2 with the remaining ye'elimite. When M-value = 2, reaction 3 occurs and no anhydrous phase remains. For M-value > 2, reaction 3 occurs and some residual anhydrite remains [41]. From these theoretical predictions, it can be hypothesised that the amount of aluminum hydroxide would be more in case of lower M-value as two AH_3 generating reactions are favoured in this case.

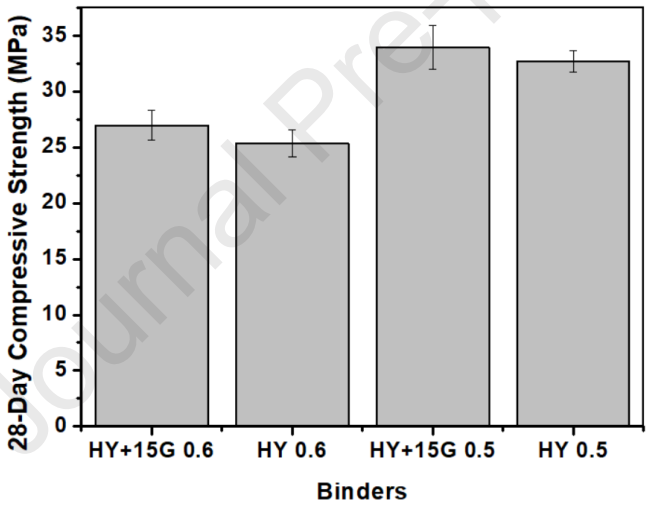

Figure 2 Influence of w/c ratio and gypsum on compressive strength of paste specimens

The effect of gypsum blending on mechanical properties of CSA cement was studied by measuring compressive strength of hydrated cement pastes (Figure 2). The addition of gypsum to CSA cement favours the formation of more space-filling ettringite over monosulfate. Higher strength of such matrix has been reported in earlier studies [9,42,43]. Although the average compressive strength of gypsum blended cement was marginally higher than CSA cement, the increase was not statistically significant. However, the effect of gypsum addition on early-age strength was not verified in this study.

199 Figure 3 shows XRD patterns of unhydrated CSA cement and hydrated CSA cement pastes with
200 and without gypsum. The XRD peaks corresponding to gypsum phase were absent in hydrated
201 CSA cement paste indicating its consumption. All hydrated systems had a large amount of
202 ettringite. The degree of hydration of ye'elimite increased as the w/c ratio increased from 0.5 to
203 0.6. This is evident from the reduction in relative intensity of ye'elimite peak.

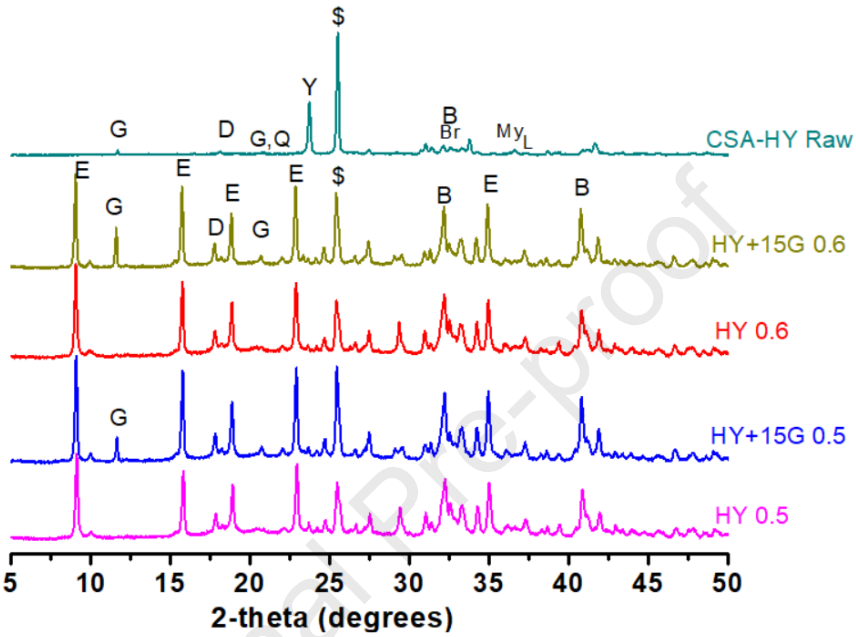

204

Figure 3 XRD patterns of 28-day hydrated binders and CSA-HY raw cement

(Note: E − Ettringite, B – Belite, Y – Ye'elimite, $ – Anhydrite, G – Gypsum, D – Dolomite, Br – Brownmillerite, L – Lime, Q – Quartz, My – Mayenite)

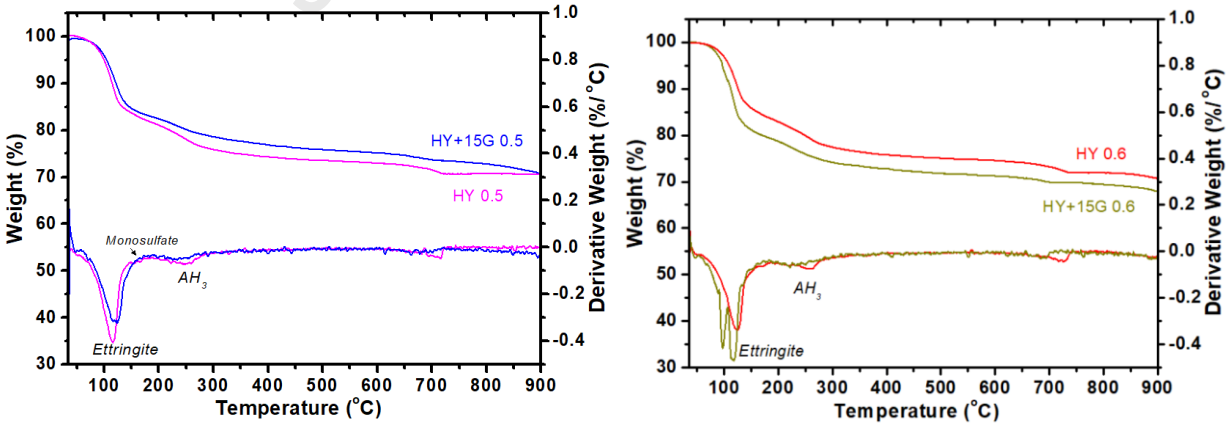

Figure 4 TG and DTG curves of 28-day cured control pastes (a) w/c = 0.5 (b) w/c = 0.6

Pure CSA cement without external gypsum is expected to have monosulfate, as evident from differential thermogravimetric (DTG) curve in Figure 4. As gypsum is added to the CSA cement, more ettringite is expected to form, making the system expansive [11,12,34]. From the TGA results, a reduction in ettringite amount was observed on gypsum blending at the w/c ratio of 0.5, possibly due to the dilution of ye'elimite [12]. However, at w/c ratio of 0.6, gypsum blend had more ettringite indicating that 0.6 was sufficient to promote reaction (3). From the TGA and XRD, it can be concluded that the major phases in hydrated CSA cement are ettringite, monosulfate, and AH_3, also observed by [34]. AH_3 is the phase having higher acid neutralization capacity (as per the reaction 1) [19,20] and its presence improves the acid resistance of the hydrated binder. All the binders show a peak around 270°C, corresponding to dehydroxylation of aluminium hydroxide [44]. Table 5 shows the mass loss due to AH_3 dehydroxylation in various binders.

Table 5 Mass loss (from TGA) due to AH_3 dehydroxylation in CSA binders

Binders	Temperature range (°C)	Mass range (%)	Mass Loss (%)
HY 0.5	175 – 341	82.2 – 75.0	7.2
HY+15G 0.5	176 – 333	83.2– 78.0	5.2
HY 0.6	184 – 352	82.3 – 75.0	7.3
HY+15G 0.6	181 – 326	79.5 – 73.7	5.8

As the effect of gypsum on strength and mineralogy was similar at both w/c ratios, further studies on acid attack were focused on the w/c ratio of 0.5 and presented in following sections.

3.2 Hydrochloric and sulfuric acid attack of binders

3.2.1 Evolution of physical changes

Changes in mass and cross-section area of specimens due to acid exposure were monitored to assess the physical damage. Figure 5(a) shows the normalized mass evolution across exposure period in 2% HCl (pH of 0.33) environment. Gypsum blended CSA system exhibited higher mass

225 loss compared to the CSA cement without additional gypsum. Within three weeks all systems
226 except HY 0.5 perished in 2% HCl environment.

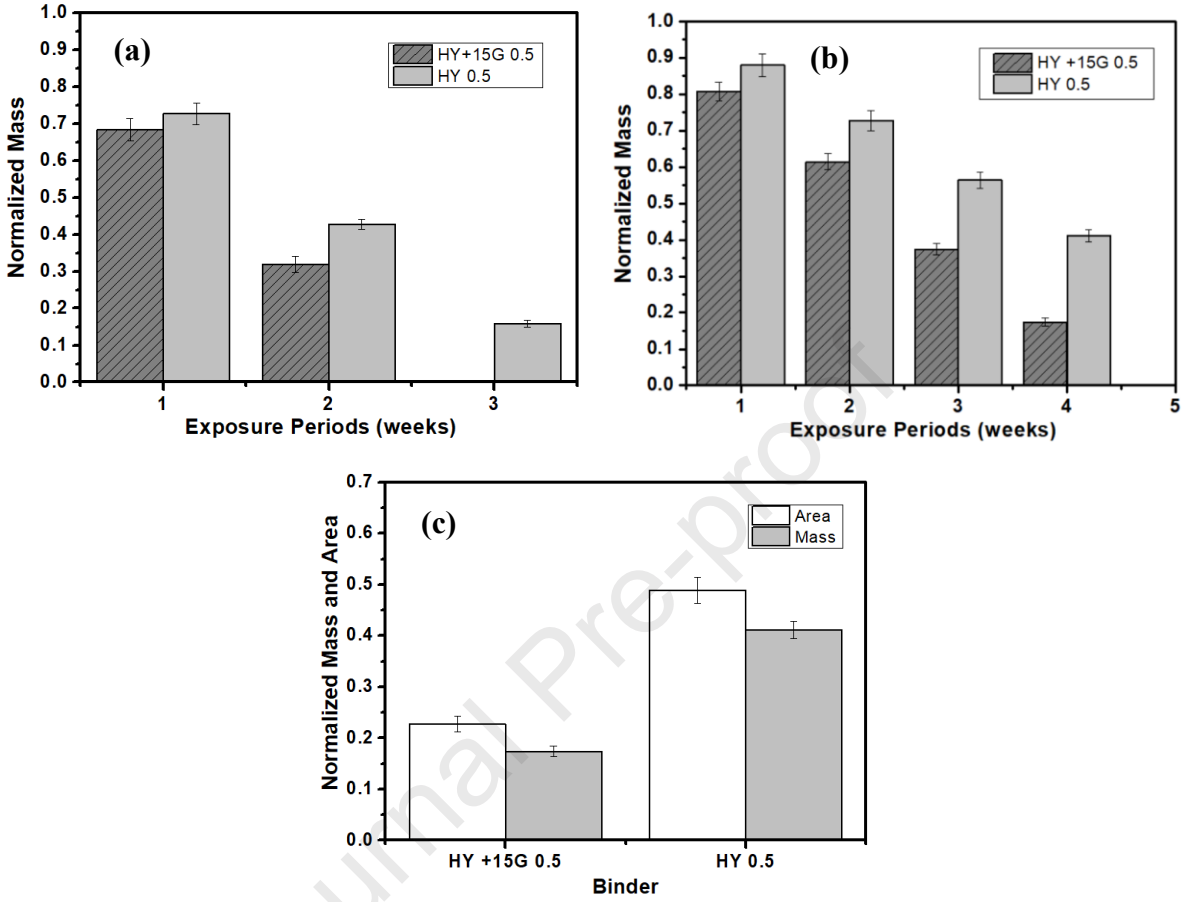

227
228

Figure 5 (a) Influence of 2% HCl attack on normalized mass with exposure time, (b) Influence of 1% HCl attack on normalized mass with exposure time, and (c) Comparison of influence of 1% HCl attack on normalized cross-sectional area and mass after four weeks of exposure

229 In order to explore the degradation kinetics, 1% of HCl (pH of 0.59) was considered. The visual
230 observation of specimens after 3 weeks of exposure is shown in Figure 6 and the mass loss results
231 are plotted in Figure 5(b). The area loss occurring in 1% HCl is represented in Figure 5(c). The
232 trend in area loss is matching with the mass loss at the end of same exposure period. The mass loss
233 and area loss for w/c – 0.6 were higher than at w/c of 0.5 (not shown here). Spalling (scaling or
234 peeling) was observed in gypsum blended CSA cement across the exposure period. However,
235 relatively less spalling was observed in control CSA cement, instead some edge cracks were
236 observed (Figure 6).

237

238

Figure 6 Specimens: HY 0.5 (left) and HY+15G 0.5 (right) after 3 weeks of exposure to 1% HCl (pH of 0.59)

239 The degradation kinetics was slower in 1% HCl compared to 2% HCl. Exceptional resistance of
240 HY 0.5 is evident in 2% (pH 0.33) (Figure 5) in the form of survival after 3 weeks and in the form
241 of lowest degradation rate in case of 1% HCl (pH 0.59). The reason could be attributed to denser
242 matrix at the lower w/c.

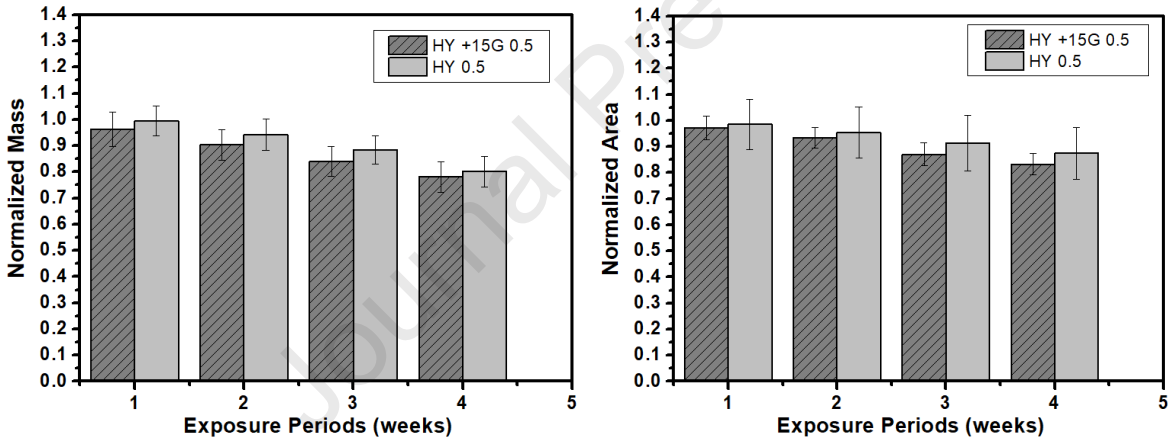

243

244 **(a)** **(b)**

Figure 7 Influence of sulfuric acid attack (2.95% conc., pH 0.5) on (a) normalized mass, and (b) normalized cross-sectional area of the binders at different exposure periods

245 Figure 7 shows that even in case of non-soluble salt forming sulfuric acid, the performance of
246 gypsum blended CSA cement followed a similar trend to the previously observed trend for HCl.
247 In sulfuric acid case, the statistical difference among the binders was not significant due to the
248 gypsum formation and the resulting pore blocking.

3.2.2 Mineralogy of acid attacked region

The main acid attack product in the case of 1% sulfuric acid attack was found to be gypsum in case of CSA and Portland cement system [32]. The same product is expected in case of 2.95% sulfuric acid (pH of 0.5) attack. Interestingly, HCl attack produced mainly gypsum and anhydrite in the case of all CSA matrices, as seen in Figure 8. The calcium sulfate salt formation in the absence of sulfate anion can be attributed to the decomposition of monosulfate and ettringite in all the CSA binders considered. Monosulfate and ettringite decomposed to form gypsum and aluminium hydroxide [32,45–49].

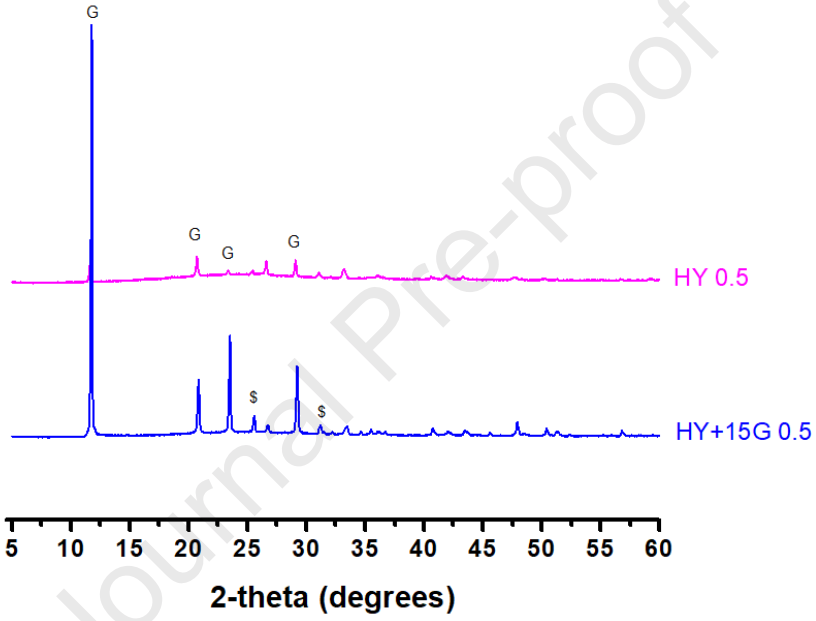

Figure 8 XRD patterns of 1% HCl attacked products (washed and filtered out) in CSA-based binders

It is worth noting that, in HCl exposure, HY+15G 0.5 showed higher intensity gypsum peaks, possibly due to residual gypsum in HY+15G (0.5). Residual gypsum may be more crystalline than secondary gypsum and thus increasing the peak intensity. In that case, residual gypsum did not provide any additional binding (as seen in Figure 10), and thus could be easily removed along with acid attack products. This could be a reason for the spalling or peeling in blend.

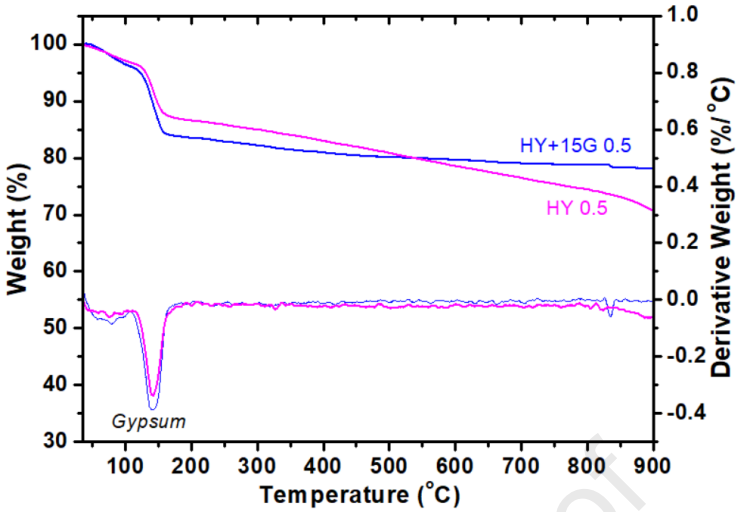

Figure 9 Thermogravimetric analysis of HCl (2% conc., pH 0.33) attack products in HY 0.5 and HY+15G 0.5 binders

From Figure 9, it was validated that the HCl acid attack product was mainly gypsum and some amount of alumina gel. The small DTG peak around 100°C can be attributed to alumina gel while crystalline aluminium hydroxide decomposes in the temperature range 210 – 300 °C [37,50]. Hence, it can be inferred that the aluminium rich decomposition product of ettringite/monosulfate was in the form of alumina gel. The gypsum amount was higher in HY+15G 0.5 which could be due to the additional contribution from the fragmented residual gypsum.

3.2.3 Morphology of the exposed surface

Morphological studies were carried out to support the findings of mineralogical investigation. SEM analysis of acid-attacked specimens is presented in this section.

2% (pH 0.33) HCl Exposed Hy +15G 0.5

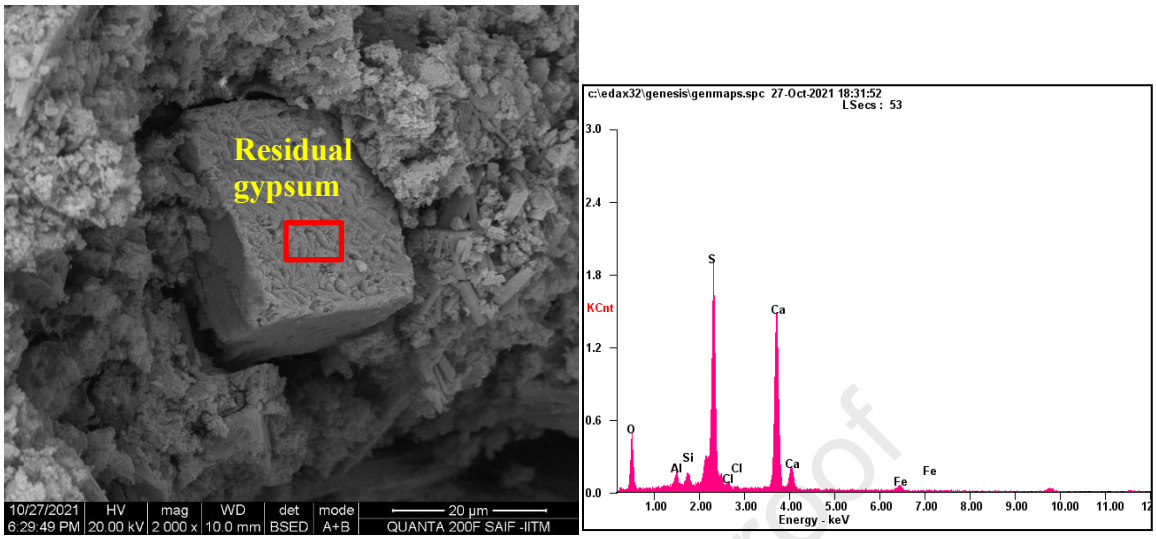

Figure 10 SEM showing residual gypsum and the EDS performed on it

Figure 10 shows the presence of residual gypsum in the HCl acid-attacked HY +15G (0.5) mix. Considering the limitations, the EDS performed on this feature showed signals mainly of Ca, S, and O. Secondary gypsum is also visible nearby. Even though the residual gypsum seems to be resistant to HCl, the pits observed around it can be formed due to leaching. The effect of decalcification [51] by the strongly decalcifying acid such as HCl is evident here [52].

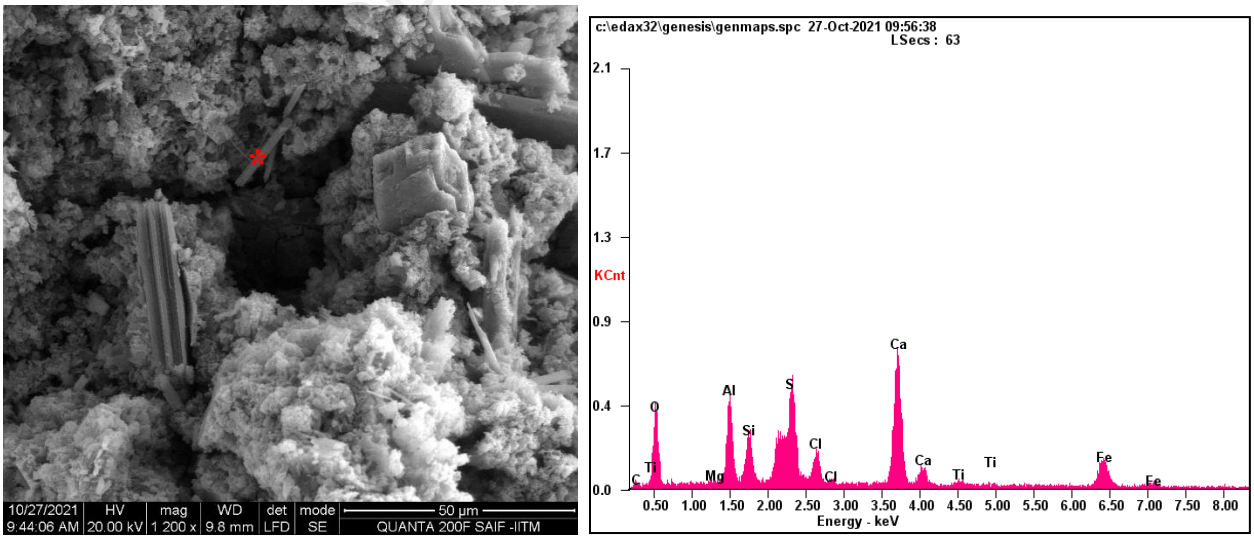

(a)

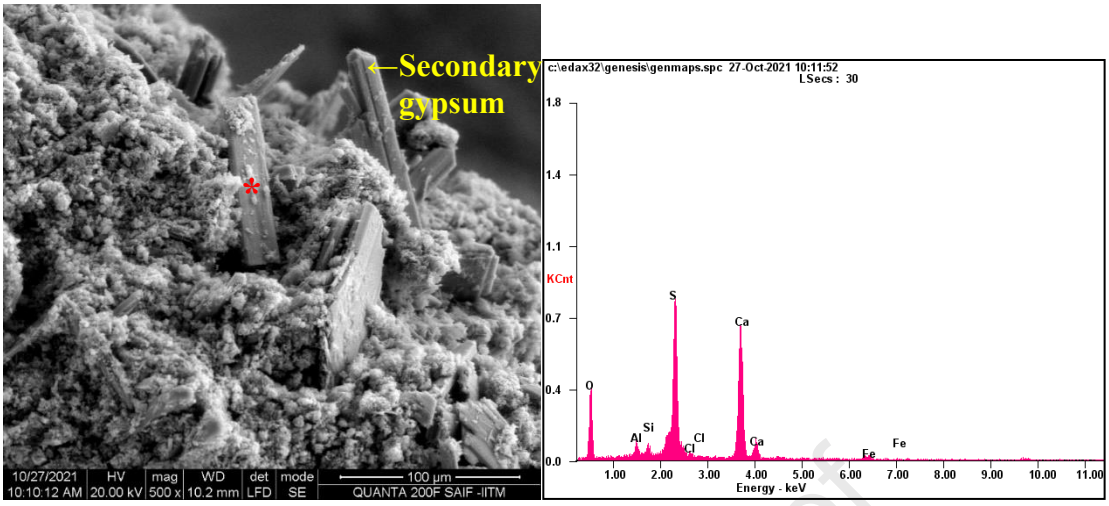

(b)

Figure 11 SEM-EDS at (a) the acid-attacked core-interface, and (b) gypsum in altered surface

Figure 11 shows the SEM - EDS of 2% HCl attacked region of Hy +15G 0.5. The EDS has peaks of Ca, S, Al, O, and Cl, initially indicating the formation of Kuzel's salt ($3CaO.Al_2O_3.0.5CaCl_2.0.5CaSO_4.10H_2O$)[53]. However, considering the needle-like morphology of the phase observed, it appeared to be chloride-modified ettringite [54]. Further, this morphology was stable at the pH of interface region. The interface was visible as a weak zone, and hence was easy to spall off (Figure 11(a)). Gypsum was visible toward the altered external surface (Figure 11(b)).

2% (pH 0.33) HCl Exposed Hy 0.5

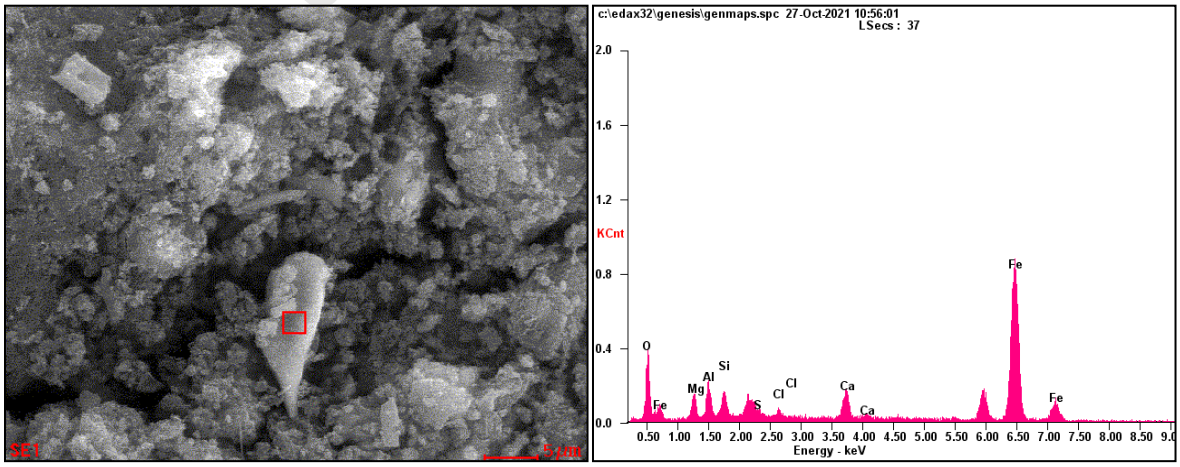

Figure 12 SEM-EDS showing iron signal indicating the resistance of iron to leaching

Figure 12 shows the traces of iron in the acid attacked HY 0.5. This iron may confer some protective action towards further attack [55]. Furthermore, the iron compound was visible in the form of brown stains in acid attacked specimens. The peaks corresponding to Fe, Al, and Si can be attributed to the less soluble hydroxides of these elements in HCl attack [56].

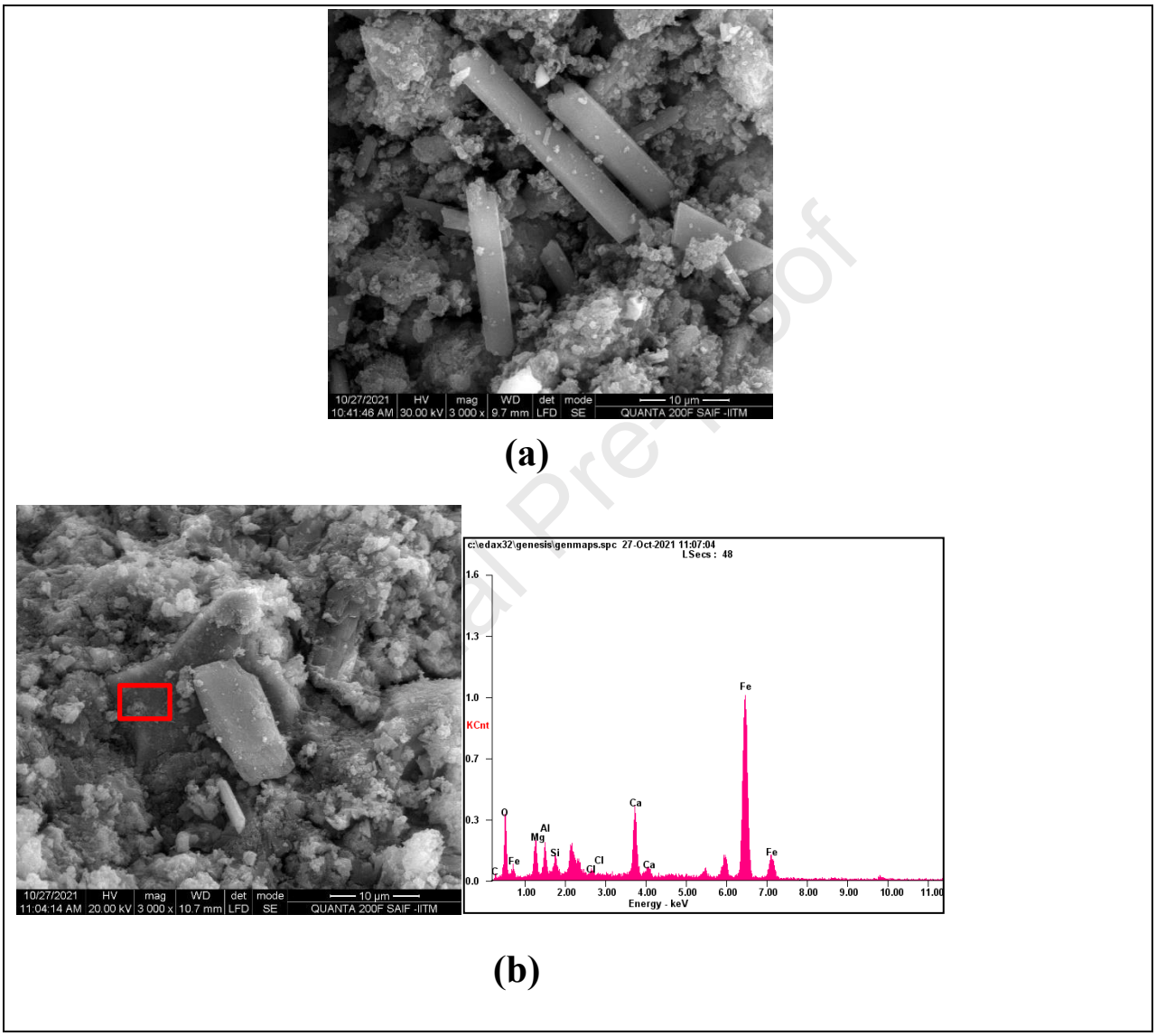

Figure 13 SEM and EDS showing acid-attacked HY 0.5 binder

Figure 13(a) shows gypsum formed and this could be encapsulated with a medium containing aluminium, silica, and magnesium as explained in [57] and possibly iron as found in the EDS Figure 13(b). Such a zone can act as a protective barrier against acid attack by preventing the acid diffusion. The Al in the EDS spectra can be attributed to the AH_3 formed by the decomposition of ettringite as explained in [32].

3.3 Evaluating acid resistance using acid consumption method

It is noted that the effect of sulfuric acid was not clearly discernable. Hence, the acid resistance was evaluated using a short-term acid neutralization test for monolithic specimens and powdered samples as reported by Damion and Chaunsali in [36] at pH of 2. The static pH test using 2.95% sulfuric acid (pH of 0.5) is difficult to be controlled because of the enormous acid consumption involved. However, static pH test is the best method for lower concentration tests such as pH 2 and above [36]. For this reason and for the fact that pH 2 was recommended in [35], static pH 2 was adopted.

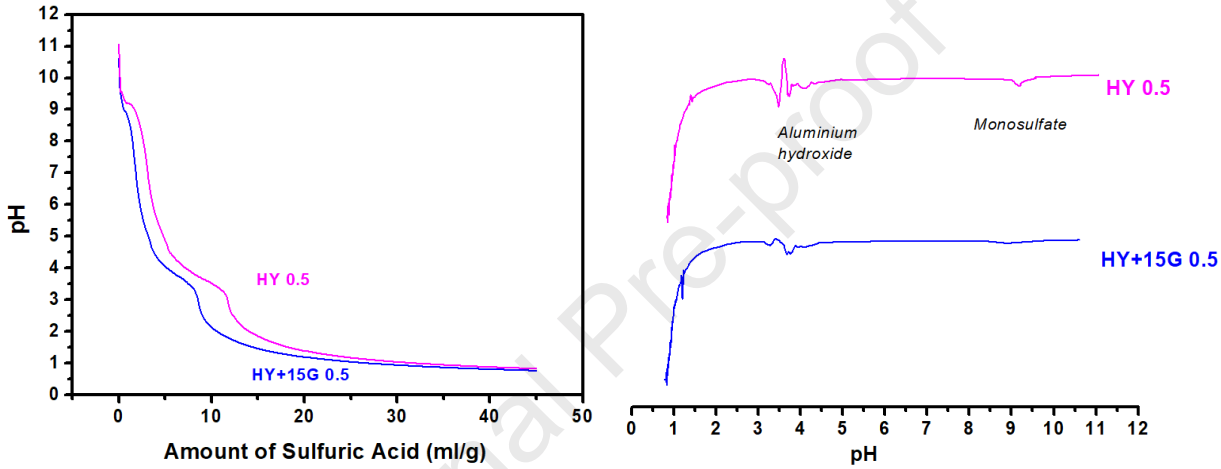

Figure 14 (a) Powder titration curve (dosing precision = 0.002 ml), and (b) differential neutralisation curve [Note: titrant was 5% sulfuric acid]

From Figure 14 (a), it is evident that there was marginal reduction in pH after gypsum addition. The pH reduced from 11.055 to 10.605. From Figure 14 (b), it can be observed that non-expansive CSA cement had prominent peaks corresponding to monosulfate and aluminium hydroxide phases. In case of expansive binder (gypsum blended CSA cement), only a feeble AH_3 peak was observed. Hence, the neutralization capacity of expansive binders is reduced due to the reduced amount of AH_3.

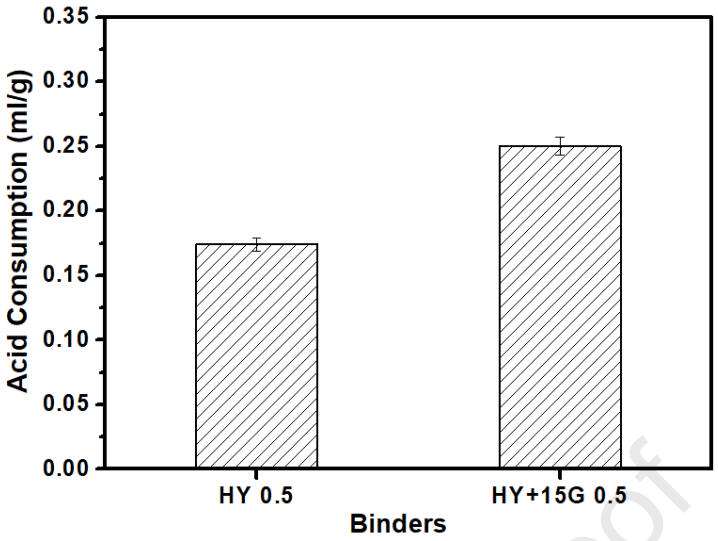

Figure 15 Acid consumption (5% sulfuric acid) of binders based on powder test [Note: acid consumption from the pH of DP to pH of 2]

As discussed in [36], the titrator stabilizing point (SP) was considered for determining acid consumption (ANC) in static pH (STAT) test as Step 1. Then, the pH corresponding to divergence point (DP) in pH vs. time curve (in STAT pH test) was identified. The corresponding acid consumption from the pH of DP to pH of 2 was determined from the titration of powders. In pH vs. time graph for static pH test of monolithic specimens, SP refers to the pH in the graph after which the pH is constant at set pH value. In the same graph, DP is the point corresponding to the maximum pH during the initial pH increment immediately after specimen acid interaction. The acid consumption in the case of powder test was determined and is presented in Figure 15. As reported by Damion and Chaunsali [36], acid consumption was found to be directly proportional to deterioration. Hence, based on acid consumption, deterioration in binders could be ranked as HY+15G 0.5 > HY 0.5. This result validates the observation from the immersion tests. Gypsum addition leads to poorer acid resistance.

Expansive CSA cement has a lower critical pore size than non-expansive CSA when expansion does not cause microcracking. However, the amount of ettringite formed and the compressive strength are similar for both systems at early ages [12]. More porous system has extra space for the expansive sulfate attack products to be deposited, which is advantageous for durability at early stage of attack [58]. In the powder test, chemical composition influences the behavior rather than critical pore size and strength. Chemical composition of the matrix is essential in assessing the

acid resistance of systems [52]. The plateau around pH of 9.15 – 9.3 (peak in differential neutralization curve) can be attributed to monosulfate degradation, thus contributing to neutralisation capacity. However, such a plateau is absent in gypsum blended systems, because of the absence of the same here. The smaller plateau length in non-expansive system could be attributed to the lower amount of monosulfate even in this case. The ettringite appears to degrade quickly, similar to portlandite, without contributing to the neutralisation capacity, though at a lower pH than monosulfate [36]. However, the occurrence of monosulfate plateau at lower pH than pH 11.6 [36,59] is not explored and could be attributed to the interaction effect due to the co-existence of monosulfate and ettringite.

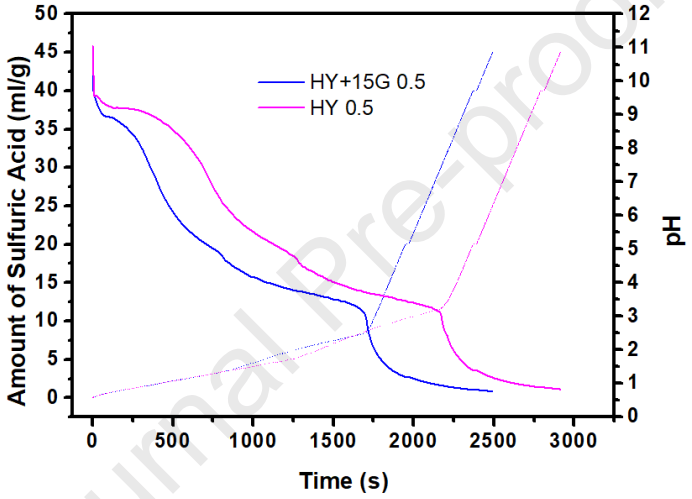

Figure 16 Sulfuric acid consumption (dotted line) and pH evolution across time.

Acidification could be delayed by more buffering action or neutralisation capacity contributed by the higher amount of AH_3 in case of non-expansive pure matrix. Further, as mentioned before, non-expansive binders have higher pore water pH, and hence the acidification was delayed, as evident from Figure 14. In view of this observations, the time factor was considered and presented in Figure 16. As a result of phase buffering and higher pore water pH, the acidification was delayed in non-expansive binders as compared to expansive system, as observed in Figure 16. This explains the early deterioration of gypsum blended expansive system in the immersion tests.

4 Discussions

The mineralogy of acid-attacked products in CSA cement is independent of anion [36]. This was further validated in this study using HCl acid. Though the anion was not sulfate but chloride, the products were predominantly gypsum and anhydrite. Hence, in CSA cement, acid attack products

354 such as gypsum and alumina gel are formed through the decomposition of monosulfate and
355 ettringite by H^+ ions of the attacking acids. When the M-value (gypsum-to-ye'elimite ratio) is high,
356 more ettringite is formed over monosulfate and the amount of aluminium hydroxide is reduced.
357 As a result, neutralization capacity of the binder is reduced. This led to superior acid resistance of
358 CSA cement without external gypsum. From the TGA results of the hydrated binders, the reduction
359 in aluminium hydroxide content on gypsum blending can be inferred. However, a slight
360 disproportionate reduction in the neutralisation capacity for AH_3 can be observed from the titration
361 curves. The ratio of mass loss in TGA corresponding to AH_3 for HY +15G 0.5 and HY 0.5 was
362 1.38. The ratio of the amount of sulfuric acid consumed in the the titration curve plateau around
363 pH 3 – 4 corresponding to AH_3, for HY 0.5 and HY+15G 0.5 was 1.14. Hence, the quantity of
364 aluminium hydroxide is mainly affecting the neutralisation capacity and the type of AH_3 may have
365 less role. However, the current study didn't validate the nature of AH_3 in different CSA cement
366 systems. The total acid consumption by the end of AH_3 decomposition for HY 0.5 was 11.2 ml/g
367 while that for HY+15G 0.5 was 8.3 ml/g. This lag was induced by the neutralisation capacity
368 offered by the monosulfate in HY 0.5, which was evident from the acid consumption 6 ml/g and
369 3.8 ml/g for HY 0.5 and HY+15G 0.5 before AH_3 decomposition.
370
371 The gypsum related deterioration can occur in the form of surface softening [45] as observed in
372 sulfuric acid attack of non-expansive CSA cement. Such a smoothening is quite evident in the
373 sulfuric acid attack of CSA cement. Specimens seemed to be pristine till the moment of brushing.
374 On brushing, one can feel the extent of surface softening in contrast to the visual judgement! The
375 layer-by-layer peeling in case of acid attack of gypsum blended CSA cement attributed to the
376 extensive gypsum formation ultimately leading to loss of adhesion [56]. This can be explained in
377 detail in a similar way as reported in [60]. The gypsum crystals are aggregated on surface and act
378 as a peel which tries to expand. However, the unattacked bulk cement paste just below tries to
379 resist expansion and this leads to the creation of resultant compressive stress. This stress causes
380 detachment of the gypsum layer. The mechanism further proceeds leading to the formation of
381 second layer and detachment (peeling), then third layer and so on. The specimens were exposed to
382 acid after 28 days, much after the expansion stabilised at around 0.17% after 10 – 15 days [12].
383 However, when specimens exposed before the age of 10 – 15 days, additional expansive stress
384 from the substrate would affect the equilibrium of stresses, resulting in different peeling

385 characteristics. This needs to be explored by conducting acid immersion at early age of specimens,
386 in addition to that with 28-day cured specimens as done in this work following ASTM C 1898.
387

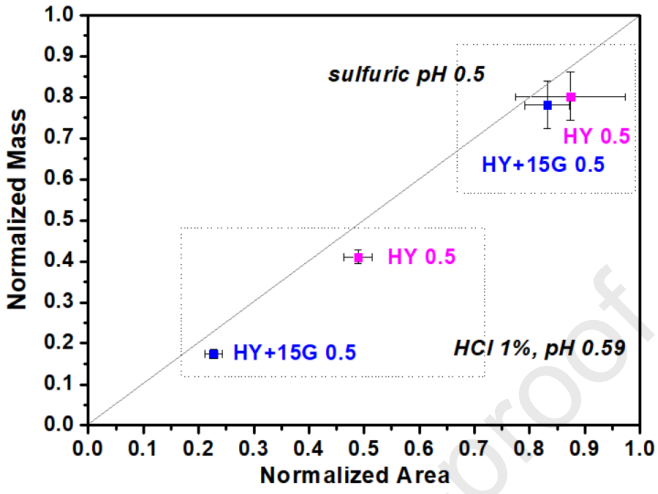

388

Figure 17 Correlation between normalized mass and cross-sectional area after four weeks of exposure in 1% HCl (pH of 0.59), and 2.95% sulfuric acid (pH of 0.5)

389 Figure 17 shows a correlation between the indicators of damage such as mass loss and section loss
390 for two acids: 1% HCl (pH of 0.59) and 2.95% H_2SO_4 (pH of 0.5). The damage was more in case
391 of 1% HCl even though it had a higher pH as compared to sulfuric acid of pH 0.5. HCl attack
392 exhibits acidolysis mechanism [33], leading to formation of soluble salts and thus the removal of
393 elements from the surface [61]. However, in sulfuric acid (pH 0.5), less soluble calcium sulfate is
394 formed and deposition of secondary products does not result material loss. Another inference is
395 that both acid attack mechanisms are limited to the surface. In 1% HCl attack, the depth of
396 degradation and neutralization was large, and leaching only occurred in this depth. The mass-loss
397 was higher than area-loss as observed in Figure 17. If mass-loss from leaching is high enough, the
398 deviation from the 1:1 line should have been more in HCl attack; however, it was similar in both
399 acids. The deviation could be mainly attributed to the damage on two end faces and the loss which
400 is not included in the cross-sectional area-loss calculations. Hence, the more damage in HCl attack
401 was due to higher section loss arising from increased depth of degradation. Along the depth,
402 leaching increases interconnected porosity and the acid attack front progresses rapidly in HCl
403 attack.

Another important observation is that the difference between acid attack performance of these binders having w/c ratio of 0.5 could not be statistically differentiated in sulfuric acid attack of pH 0.5. This was due to the saturation of sulfuric acid solution with calcium sulfate and the followed precipitation over same specimen surface in one-week time between renewal. In fact, in biogenic sulfuric acid attack experienced in a live sewer, the gypsum layer gets eroded or dissolved. The remedy for this is that chemical acid resistance study should be performed by acids such as HCl forming soluble salts [62]. Hence, HCl acid attack can help in differentiating the binders as well as imitate field scenario as per [62]. However, the acid attack product mineralogy would be different for portlandite containing binders in HCl acid attack, if field imitation is considered. In this situation, sulfuric acid attack test method using the autotitrator helped and the gypsum blend found to have more damage than pure CSA matrix. In spite of having marginally higher strength of gypsum blended CSA cement, its acid resistance was found to be poorer.

5 Conclusions

Main conclusions of the study are summarized below:

- Gypsum blending in a ye'elimite rich CSA cement used in this study led to poorer acid resistance. Poorer resistance of gypsum blended CSA cement was due to reduced amount of aluminium hydroxide and monosulfate.
- The acid consumption was found to be a suitable indicator to differentiate CSA cement with and without gypsum.
- The deterioration associated with 1% HCl acid attack was higher than 2.95% sulfuric acid attack in spite of lower concentration of HCl. This could be attributed to the leaching-dominated mechanism in hydrochloric acid attack and gypsum precipitation in sulfuric acid attack.

6 Acknowledgements

The first author would like to acknowledge the doctoral scholarship received from the Ministry of Human Resource Development (MHRD), India. All authors would like to acknowledge the resources provided by the Department of Civil Engineering at the Indian Institute of Technology (IIT) Madras towards the usage of experimental facilities in this study. The last author is also grateful for the financial support from the New Faculty Seed Grant (CE1920426NFSC008926) by Industrial Consultancy and Sponsored Research (ICSR) centre at IIT Madras. The Institute of

Eminence Research Initiative project grant on Technologies for Low Carbon and Lean Construction from IIT Madras is also gratefully acknowledged.

7 References

[1] T. Hanein, J.L. Galvez-Martos, M.N. Bannerman, Carbon footprint of calcium sulfoaluminate clinker production, J. Clean. Prod. 172 (2018). https://doi.org/10.1016/j.jclepro.2017.11.183.

[2] W.H. Olmstead, H. Hamlin, Converting Portions of the Los Angeles Outfall Sewer into a Septic Tank, Eng. News Am. Railw. J. XLIV (1900) 317–318. www.sewerhistory.org/articles/trtmnt/1900_aen18/article.pdf%5CnCached%5Cn.

[3] C. Parker, The Corrosion of Concrete: 1. The Isolation of a Species of Bacterium Associated With the Corrosion of Concrete Exposed To Atmospheres Containing Hydrogen Sulphide., Aust. J. Exp. Biol. Med. Sci. 23 (1945) 81–90. https://doi.org/10.1038/icb.1945.13.

[4] C. Parker, The Corrosion of Concrete: 2. The Function of Thiobacillus Concretivorus (Nov. Spec.) in the Corrosion of Concrete Exposed To Atmospheres Containing Hydrogen Sulphide., Aust. J. Exp. Biol. Med. Sci. 23 (1945) 91–98. https://doi.org/10.1038/icb.1945.14.

[5] J. Bensted, A.R. Brough, M.M. Page, Chemical degradation of concrete, Durab. Concr. Cem. Compos. (2007) 86–135. https://doi.org/10.1533/9781845693398.86.

[6] W. Zhang, S. Gong, B. Kang, Surface Corrosion and Microstructure Degradation of Calcium Sulfoaluminate Cement Subjected to Wet-Dry Cycles in Sulfate Solution, Adv. Mater. Sci. Eng. 2017 (2017) 1–8.

[7] J. Beretka, M. Marroccoli, N. Sherman, G.L. Valenti, The influence of C4A3S̄ content and W/S ratio on the performance of calcium sulfoaluminate-based cements, Cem. Concr. Res. 26 (1996) 1673–1681. https://doi.org/10.1016/S0008-8846(96)00164-0.

[8] Y. Jeong, C.W. Hargis, S.C. Chun, J. Moon, The effect of water and gypsum content on strätlingite formation in calcium sulfoaluminate-belite cement pastes, Constr. Build. Mater. 166 (2018). https://doi.org/10.1016/j.conbuildmat.2018.01.153.

[9] M. Mrak, F. Winnefeld, B. Lothenbach, S. Dolenec, The influence of calcium sulfate content on the hydration of belite-calcium sulfoaluminate cements with different clinker phase compositions, Mater. Struct. Constr. 54 (2021). https://doi.org/10.1617/s11527-021-

01811-w.

[10] Liang. Zhang, Microstructure and performance of calcium sulfoaluminate cements, 2000.

[11] F. Winnefeld, S. Barlag, Calorimetric and thermogravimetric study on the influence of calcium sulfate on the hydration of ye'elimite, J. Therm. Anal. Calorim. 101 (2010) 949–957. https://doi.org/10.1007/s10973-009-0582-6.

[12] V.K. Shenbagam, P. Chaunsali, Influence of calcium hydroxide and calcium sulfate on early-age properties of non-expansive calcium sulfoaluminate belite cement, Cem. Concr. Compos. 128 (2022) 104444. https://doi.org/10.1016/j.cemconcomp.2022.104444.

[13] F. Bullerjahn, J. Skocek, M. Ben, K. Scrivener, Chemical shrinkage of ye ' elimite with and without gypsum addition, Constr. Build. Mater. 200 (2019) 770–780. https://doi.org/10.1016/j.conbuildmat.2018.12.170.

[14] F. Bullerjahn, E. Boehm-Courjault, M. Zajac, M. Ben Haha, K. Scrivener, Hydration reactions and stages of clinker composed mainly of stoichiometric ye'elimite, Cem. Concr. Res. 116 (2019) 120–133. https://doi.org/10.1016/j.cemconres.2018.10.023.

[15] G.C. Bye, J.G. Robinson, Crystallization Processes in Aluminium Hydroxide Gels, Kolloid-Zeit Zeit Fuer Polym. 198 (1963) 53–60. https://doi.org/10.1007/BF01499454.

[16] H. De Hek, R.J. Stol, P.L. De Bruyn, Hydrolysis-precipitation studies of aluminum(III) solutions. 3. The role of the sulfate ion, J. Colloid Interface Sci. 64 (1978) 72–89. https://doi.org/10.1016/0021-9797(78)90336-3.

[17] A. Allahverdi, F. Škvára, Acidic corrosion of hydrated cement based materials. Part 1. Mechanism of the phenomenon, Ceram. - Silikaty. 44 (2000) 114–120.

[18] V. Pavlík, Corrosion of hardened cement paste by acetic and nitric acids part II: Formation and chemical composition of the corrosion products layer, Cem. Concr. Res. 24 (1994) 1495–1508. https://doi.org/10.1016/0008-8846(94)90164-3.

[19] K.L. Scrivener, J.L. Cabiron, R. Letourneux, High-performance concretes from calcium aluminate cements, Cem. Concr. Res. 29 (1999) 1215–1223. https://doi.org/10.1016/S0008-8846(99)00103-9.

[20] T. Dyer, Influence of cement type on resistance to attack from two carboxylic acids, Cem. Concr. Compos. 83 (2017) 20–35. https://doi.org/10.1016/j.cemconcomp.2017.07.004.

[21] N. Ukrainczyk, M. Muthu, O. Vogt, E. Koenders, Geopolymer, calcium aluminate, and portland cement-based mortars: Comparing degradation using acetic acid, Materials

(Basel). 12 (2019). https://doi.org/10.3390/ma12193115.

[22] M.W. Kiliswa, K.L. Scrivener, M.G. Alexander, The corrosion rate and microstructure of Portland cement and calcium aluminate cement-based concrete mixtures in outfall sewers: A comparative study, Cem. Concr. Res. 124 (2019) 105818. https://doi.org/10.1016/j.cemconres.2019.105818.

[23] J. Herisson, M. Guéguen-Minerbe, E.D. Van Hullebusch, T. Chaussadent, Behaviour of different cementitious material formulations in sewer networks, Water Sci. Technol. 69 (2014) 1502–1508. https://doi.org/10.2166/wst.2014.009.

[24] A. Grandclerc, P. Dangla, M. Gueguen-Minerbe, T. Chaussadent, Modelling of the sulfuric acid attack on different types of cementitious materials, Cem. Concr. Res. 105 (2018) 126–133. https://doi.org/10.1016/j.cemconres.2018.01.014.

[25] C. Shi, J.A. Stegemann, Acid corrosion resistance of different cementing materials, Cem. Concr. Res. 30 (2000) 803–808. https://doi.org/10.1016/S0008-8846(00)00234-9.

[26] F. Winnefeld, B. Lothenbach, Hydration of calcium sulfoaluminate cements - Experimental findings and thermodynamic modelling, Cem. Concr. Res. 40 (2010) 1239–1247. https://doi.org/10.1016/j.cemconres.2009.08.014.

[27] I.A. Chen, C.W. Hargis, M.C.G. Juenger, Understanding expansion in calcium sulfoaluminate-belite cements, Cem. Concr. Res. 42 (2012) 51–60. https://doi.org/10.1016/j.cemconres.2011.07.010.

[28] E. Dan, I. Janotka, Chemical resistance of Portland cement, blast- furnace slag Portland cement and sulphoaluminate-belite cement in acid, chloride and sulphate solution: Some preliminary results, Ceram. - Silikaty. 47 (2003) 141–148.

[29] R. Cao, J. Yang, G. Li, F. Liu, M. Niu, W. Wang, Resistance of the composite cementitious system of ordinary Portland/calcium sulfoaluminate cement to sulfuric acid attack, Constr. Build. Mater. 329 (2022) 127171. https://doi.org/10.1016/j.conbuildmat.2022.127171.

[30] A.T. Bakera, M.G. Alexander, Sewer concrete subjected to biogenic acid corrosion: analysis of concrete deterioration phases using QEMSCAN, in: MATEC Web Conf. Int. Conf. Concr. Repair, Rehabil. Retrofit. (ICCRRR 2022), 2022: p. 03012. https://doi.org/10.1051/matecconf/202236403012.

[31] X. Li, X. Lin, K. Lin, T. Ji, Study on the degradation mechanism of sulphoaluminate cement sea sand concrete eroded by biological sulfuric acid, Constr. Build. Mater. 157 (2017) 331–

336. https://doi.org/10.1016/j.conbuildmat.2017.08.172.

[32] T. Damion, R. Cepuritis, P. Chaunsali, Sulfuric acid and citric acid attack of calcium sulfoaluminate-based binders, Cem. Concr. Compos. 130 (2022) 104524. https://doi.org/10.1016/j.cemconcomp.2022.104524.

[33] T. Dyer, Influence of cement type on resistance to organic acids, Mag. Concr. Res. (2016) 1–26.

[34] A. Telesca, M. Marroccoli, M.L. Pace, M. Tomasulo, G.L. Valenti, P.J.M. Monteiro, A hydration study of various calcium sulfoaluminate cements, Cem. Concr. Compos. 53 (2014). https://doi.org/10.1016/j.cemconcomp.2014.07.002.

[35] ASTM C1898, Standard Test Methods for Determining the Chemical Resistance of Concrete Products to Acid Attack, ASTM Int. (2020) 9–10. https://doi.org/10.1520/D1898-20.1.

[36] T. Damion, P. Chaunsali, Evaluating Acid Resistance of Portland Cement, Calcium Aluminate Cement, and Calcium Sulfoaluminate Based Cement Using Acid Neutralisation, Cem. Concr. Res. 162 (2022) 1–17. https://doi.org/10.2139/ssrn.4165828.

[37] P. Wang, N. Li, L. Xu, Hydration evolution and compressive strength of calcium sulphoaluminate cement constantly cured over the temperature range of 0 to 80 °C, Cem. Concr. Res. 100 (2017) 203–213. https://doi.org/10.1016/j.cemconres.2017.05.025.

[38] M. Collepardi, R. Turriziani, A. Marcialis, The paste hydration of 4CaO·3Al2O3·SO3 in presence of calcium sulphate, tricalcium silicate and dicalcium silicate, Cem. Concr. Res. 2 (1972) 213–223. https://doi.org/10.1016/0008-8846(72)90043-9.

[39] A. Bentur, M. Ish-Shalom, Properties of type K expansive cement of pure components IV. hydration of mixtures of C3S with pure expansive component, Cem. Concr. Res. 5 (1975) 597–606. https://doi.org/10.1039/b507188g.

[40] B. Lothenbach, L. Pelletier-Chaignat, F. Winnefeld, Stability in the system CaO-Al2O3-H2O, Cem. Concr. Res. 42 (2012) 1621–1634. https://doi.org/10.1016/j.cemconres.2012.09.002.

[41] T. Desbois, R. Le Roy, A. Pavoine, G. Platret, A. Feraille, A. Alaoui, Effect of gypsum content on sulfoaluminate mortars stability, Eur. J. Environ. Civ. Eng. 14 (2010) 579–597. https://doi.org/10.3166/ejece.14.579-597.

[42] F. Winnefeld, S. Barlag, Influence of calcium sulfate and calcium hydroxide on the

hydration of calcium sulfoaluminate clinker, ZKG Int. 62 (2009) 42–5 3.

[43] R. Trauchessec, J.M. Mechling, A. Lecomte, A. Roux, B. Le Rolland, Hydration of ordinary Portland cement and calcium sulfoaluminate cement blends, Cem. Concr. Compos. 56 (2015) 106–114. https://doi.org/10.1016/j.cemconcomp.2014.11.005.

[44] B. Lothenbach, P. Durdzi, K. De Weerdt, Thermogravimetric analysis, in: A Pract. Guid. to Microstruct. Anal. Cem. Mater., 2016: pp. 177–212.

[45] M. Santhanam, M.D. Cohen, J. Olek, Sulfate attack research - whither now ?, Cem. Concr. Res. 31 (2001) 845–851.

[46] C.J. Warren, E.J. Reardon, The solubility of ettringite at 25°C, Cem. Concr. Res. 24 (1994) 1515–1524. https://doi.org/10.1016/0008-8846(94)90166-X.

[47] C.W. Hargis, B. Lothenbach, C.J. Müller, F. Winnefeld, Carbonation of calcium sulfoaluminate mortars, Cem. Concr. Compos. 80 (2017) 123–134. https://doi.org/10.1016/j.cemconcomp.2017.03.003.

[48] T.Nishikawa, K.Suzuki, S.Ito, Decomposition of synthesized ettringite by carbonation, 22 (1992) 6–14.

[49] C. Xiaorong, Kinetic study of ettringite carbonation reaction, Cem. Concr. Res. 24 (1994) 1383–1389.

[50] F.A. Cardoso, M.D.M. Innocentini, M.M. Akiyoshi, V.C. Pandolfelli, Effect of curing time on the properties of CAC bonded refractory castables, J. Eur. Ceram. Soc. 24 (2004) 2073–2078. https://doi.org/10.1016/S0955-2219(03)00371-6.

[51] A. Bertron, J. Duchesne, G. Escadeillas, Attack of cement pastes exposed to organic acids in manure, Cem. Concr. Compos. 27 (2005) 898–909. https://doi.org/10.1016/j.cemconcomp.2005.06.003.

[52] O. Oueslati, J. Duchesne, Resistance of blended cement pastes subjected to organic acids: Quantification of anhydrous and hydrated phases, Cem. Concr. Compos. 45 (2014) 89–101. https://doi.org/10.1016/j.cemconcomp.2013.09.007.

[53] F.P. Glasser, A. Kindness, S.A. Stronach, Stability and solubility relationships in AFm phases. Part I. Chloride, sulfate and hydroxide, Cem. Concr. Res. 29 (1999) 861–866. https://doi.org/10.1016/S0008-8846(99)00055-1.

[54] M.V.A. Florea, H.J.H. Brouwers, Chloride binding related to hydration products: Part I: Ordinary Portland Cement, Cem. Concr. Res. 42 (2012) 282–290.

https://doi.org/10.1016/j.cemconres.2011.09.016.

[55] S. Chandra, Hydrochloric acid attack on cement mortar - An analytical study, Cem. Concr. Res. 18 (1988) 193–203. https://doi.org/10.1016/0008-8846(88)90004-X.

[56] D. Israel, D.E. Macphee, E.E. Lachowski, Acid attack on pore-reduced cements, J. Mater. Sci. 32 (1997) 4109–4116. https://doi.org/10.1023/A:1018610109429.

[57] M.T. Bassuoni, M.L. Nehdi, Resistance of self-consolidating concrete to sulfuric acid attack with consecutive pH reduction, Cem. Concr. Res. 37 (2007) 1070–1084. https://doi.org/10.1016/j.cemconres.2007.04.014.

[58] T. Ikumi, S.H.P. Cavalaro, I. Segura, The role of porosity in external sulphate attack, Cem. Concr. Compos. 97 (2019) 1–12. https://doi.org/10.1016/j.cemconcomp.2018.12.016.

[59] A. Gabrisová, J. Havlica, S. Sahu, Stability of calcium sulphoaluminate hydrates in water solutions with various pH values, Cem. Concr. Res. 21 (1991) 1023–1027. https://doi.org/10.1016/0008-8846(91)90062-M.

[60] Z. Liu, X. Li, D. Deng, The damage of calcium sulfoaluminate cement paste partially immersed in MgSO4 solution, Mater. Struct. (2016) 719–727. https://doi.org/10.1617/s11527-015-0532-7.

[61] J. Temuujin, A. Minjigmaa, M. Lee, N. Chen-Tan, A. Van Riessen, Characterisation of class F fly ash geopolymer pastes immersed in acid and alkaline solutions, Cem. Concr. Compos. 33 (2011) 1086–1091. https://doi.org/10.1016/j.cemconcomp.2011.08.008.

[62] M.G. Alexander, C. Fourie, Performance of sewer pipe concrete mixtures with portland and calcium aluminate cements subject to mineral and biogenic acid attack, Mater. Struct. Constr. 44 (2011) 313–330. https://doi.org/10.1617/s11527-010-9629-1.

Declaration of interests

☒ The authors declare that they have no known competing financial interests or personal relationships that could have appeared to influence the work reported in this paper.

☐ The authors declare the following financial interests/personal relationships which may be considered as potential competing interests: